

Article

# Distribution of Urban Blue and Green Space in Beijing and Its Influence Factors

Haoying Wang <sup>1,2</sup> , Yunfeng Hu <sup>1,3,\*</sup> , Li Tang <sup>1,2</sup> and Qi Zhuo <sup>2</sup>

<sup>1</sup> State Key Laboratory of Resources and Environmental Information System, Institute of Geographic Sciences and Natural Resources Research, Chinese Academy of Sciences, Beijing 100101, China; why93523@163.com (H.W.); tangli\_77@163.com (L.T)

<sup>2</sup> School of Civil Engineering and Architecture, Jishou University, Zhangjiajie 427000, China; zhaoqi196209@163.com

<sup>3</sup> College of Resources and Environment, University of Chinese Academy of Sciences, Beijing 100049, China

\* Correspondence: huyf@reis.ac.cn

Received: 7 February 2020; Accepted: 11 March 2020; Published: 13 March 2020



**Abstract:** Urban blue and green space is a key element supporting the normal operation of urban landscape ecosystems and guaranteeing and improving people's lives. In this paper, 97.1k photos of Beijing were captured by using web crawler technology, and the blue sky and green vegetation objects in the photos were extracted by using the Image Cascade Network (ICNet) neural network model. We analyzed the distribution characteristics of the blue–green space area proportion index and its relationships with the background economic and social factors. The results showed the following. (1) The spatial distribution of Beijing's blue–green space area proportion index showed a pattern of being higher in the west and lower in the middle and east. (2) There was a positive correlation between the satellite remote sensing normalized difference vegetation index (NDVI) and the proportion index of green space area, but the fitting degree of geospatial weighted regression decreased with an increasing analysis scale. (3) There were differences in the relationship between the housing prices in different regions and the proportion index of blue–green space, but the spatial fitting degree of the two increased with the increase of study scale. (4) There was a negative correlation between the proportion index of blue–green space and population density, and the low-population areas per unit blue–green space were mainly distributed in the south of the city and the urban fringe areas beyond the Third Ring Road. The urban blue–green space analysis that was constructed by this study provides new aspect for urban landscape ecology study, and the results proposed here also provide support for government decision-makers to optimize urban ecological layouts.

**Keywords:** urban ecology; blue sky; green vegetation; street view photo; neural network; scale effect

## 1. Introduction

In 2012, the United Nations Conference on Sustainable Development (Rio + 20) advocated for the construction of “green cities” around the world. One key component of green city construction is to plan and create an ecological space where people and nature live in harmony to ensure that the city is energy efficient, livable, and sustainable [1]. In the past ten years, the managers and occupants of Chinese cities have paid increasing attention to the construction of good ecological spaces in their cities. In 2018, Beijing revised the “Regulations on the Management of Plaque Signs in Beijing” and implemented the “Skyline Project” to create a broader sky view for citizens. Surveys from the private sector have shown that more than 56% of citizens in Beijing would like to pay more for good ecological environments. An open blue sky and pleasing green vegetation in cities (hereinafter referred to as urban blue–green space) have become common aspirations of city managers and urban citizens.

As an important component of urban landscape ecology, urban blue and green space is a key element to support the normal operation of urban landscape ecosystems and ensure and improve citizens' quality of life [2–4]. Blue–green space provides citizens with a variety of ecological spaces, enhances various services of the urban ecosystem, reduces the risk of natural disasters, and, more importantly, can improve and enhance the physical and mental health of residents [5–8]. A lot of studies exist that have investigated the distribution pattern of urban blue–green space, analyzed the spatial rules of differences in blue–green space, and summarized the relationship between blue–green space, natural geographical factors, and economic and social factors. This topic is of great significance to city planners, builders, and residents.

Traditionally, the extraction of urban blue–green space information has mainly been achieved through high-resolution satellite remote sensing monitoring and urban three-dimensional measurements. Hu [9] applied Landsat and GF-1 (or Gaofen-1, i.e., high-resolution in Chinese) imagery and used the support vector machine (SVM) method to extract urban green space indicators, e.g., urban vegetation coverage (%) and the normalized difference vegetation index (NDVI). Puissant [10] used QuickBird images with a spatial resolution of 2.4 m and applied random forest (RF) classification and object-oriented image analysis methods to monitor changes of green space in Strasbourg, France. Schreyer [11] simulated a 3D vegetation model based on 3D point cloud data from drone detectors, and the results showed that drones were suitable for the study of heterogeneous urban green spaces. Liu [12] also carried out drone experiments in the Meishan area of Ningbo city, showing that the maximum likelihood classification method and the normalized green-red difference index had the highest accuracy on assessing urban green space. In terms of the extraction of urban blue-sky space, Zhang [13] calculated sky openness based on a 3D modeling method from DTM (Digital Terrain Model) data with high-resolution building information. Shibasaki [14] used the vehicular LiDAR (Light Detection And Ranging) measurement system to calculate urban sky openness.

Typically, urban green space study requires satellite imagery with high spatial and temporal resolutions (e.g., SPOT, QuickBird, or centimeter-scale drone imagery). Currently, the widely used and free charged data (mainly 30 m resolution Landsat TM, ETM+) are not suitable for precise urban studies. The analysis process of urban sky breadth based on LiDAR data is complex and inefficient; thus, it is difficult to popularize in less developed countries and regions around the world. In addition, due to air traffic control and safety reasons, unmanned aerial vehicle (UAV) monitoring is also prohibited in many cities and regions. More importantly, less connection exists between the “top down” bird's-eye view of satellites (or drones) and the horizontal human's-eye view of the citizens. Therefore, due to a lack of earth observation data with high spatial and temporal resolutions, the spatial–temporal pertinence and validity of the research results are greatly reduced, while the difference in observation perspectives makes it difficult to guide the urban ecological construction with “people-oriented” interests.

Since 2000, with the popularity of smart phones and other smart mobile terminals, researchers have been able to obtain urban blue–green space information with field surveys by using digital cameras or mobile phones to take photos, and then they have been able to carry out in-depth studies on the scale of streets and communities [15,16]. However, the number of photos in individual experiments is always ultimately limited, and methods based on human visual interpretation are extremely time-consuming. Therefore, it is difficult to apply these methods to the urban scale and even more difficult to apply them to the national scale [17,18]. However, many internet information service companies, represented by Google, Bing, Baidu and Tencent, have accumulated giant street view photos by sending information collection vehicles to conduct cruise surveys and take panoramic photographs in major cities around the world. For example, by 2019, Baidu Map had collected street view photos in 372 Chinese cities, with the total capacity of street view photos exceeding 700 TB [19]. These street view photos have omni-directional and multi-angle characteristics. Based on the timestamp information of street view photos, the dynamic changes of city can be further analyzed. It is convenient to explore all imagery in different locations, and the cost to obtain and download the imagery is almost zero. It is an important and fundamental way forward urban studies to make full use of satellite images and street view photos.

In addition, the artificial intelligence technology makes it possible to extract information from the massive amount of satellite images and street view photos. In the past five years, researchers have made great progress. In terms of the information extraction from satellite imagery, based on convolutional neural network (CNN) model, cross-band information integration and average pooling methods, Hu [20] carried out land cover classification in Qinhuangdao City and achieved good results. Supported by the high-quality large-scale radar target sample dataset, Chen [21] used deep learning for target recognition on SAR (Synthetic Aperture Radar) images and improved detection accuracy. Navickas [22] pointed out that the visual quality of urban landscapes has important impacts on the mental health and well-being of urban residents. The CLM (contemplative landscape model) is a useful and operational tool to assess these impacts. The most important contribution is that they provided a potential framework for future studies. In terms of the information extraction from street view photos, Wang [23] used the FCN-8s (Fully Convolutional Network) neural network model to extract the information and further analyzed the relationship between the health of elderly people and urban blue–green space. In general, there is no doubt that the application of artificial intelligence technology in traditional geoscience studies—e.g., satellite imagery land interpretation, high-value object identification, urban functional zoning, and city landscape evaluation—have become important directions. Some researchers have begun to use street photographs to extract urban blue–green space information. However, most existing studies are simply and qualitatively described relationships between urban blue–green space and residents' health. There is little knowledge about the multi-scale distribution rules of urban blue–green space, and the quantitative relationship between urban blue–green space and background factors has been very rarely discussed.

In view of the above problems, the authors planned to apply internet big data and image recognition technology supported by artificial intelligence to extract urban blue–green space information. The authors attempted to characterize the spatial distribution pattern of blue–green space in Beijing. Additionally, this study explores the relationships between blue–green space and satellite remote sensing indicators, urban housing prices, and population density. The authors tried to answer the following three questions:

1. How do we construct a technique flowchart and practical system to extract blue–green space information?
2. What are the spatial distribution patterns of urban blue–green space in Beijing, China?
3. What are the quantitative relationships between blue–green space and environmental and social–economic factors?

## 2. Study Areas, Data and Methods

### 2.1. Study Area

Beijing, the capital and political, cultural, economic, scientific, and technological innovation center of China, is located in Northern China (116°20' E, 39°56' N) (Figure 1). Beijing is not only a world-famous ancient capital but also a modern international city. In 2016, Beijing was ranked second among all Chinese cities according on the United Nations human development index. In 2017, it was ranked as a global first-class city by the Globalization and World Cities (GaWC) [24]. According on the China Statistical Yearbook 2018, the permanent population of Beijing is 21.54 million, with a GDP of RMB 3,032 billion [25]. The climate of Beijing is a typical, sub-humid, continental monsoon climate in the warm temperate zone. The summer is hot and rainy, the winter is cold and dry, and the spring and autumn have short durations.

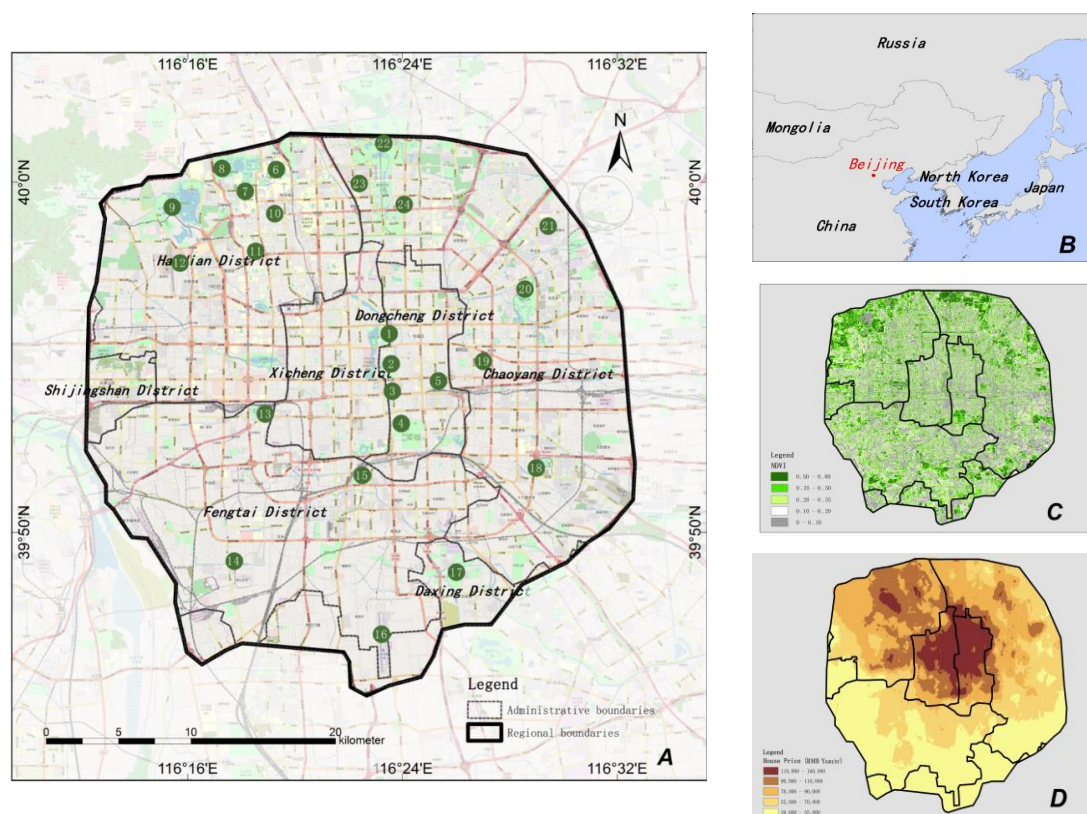


**Figure 1.** Location, scope and backgrounds of the study area. (A) Twenty-four reference landmarks (1, Beihai Park; 2, Forbidden City; 3, Tiananmen Square; 4, Tiantan Park; 5, Beijing Station; 6, Tsinghua University; 7, Peking University; 8, Yuanmingyuan Imperial Garden; 9, Summer Palace; 10, Zhongguancun; 11, China Renmin University; 12, Beijing Xijiao Airport; 13, Beijing West Station; 14, Fengtai Science and Technology Park; 15, Beijing South Station; 16, Beijing Nanyuan Airport; 17, Wangxing Lake Country Park; 18, Happy Valley; 19, Beijing World Financial Center; 20, Chaoyang Park; 21, Beijing 798 Art District; 22, Olympic Park; 23, Olympic Village; and 24, Asian Games Village); (B) the location of the study area in East Asia; (C) the spatial distribution of the Sentinel-based normalized difference vegetation index (NDVI) in 2017; and (D) spatial distribution of house prices at the end of 2019.

In this study, the core urban area of Beijing—the area within the Fifth Ring Road of the urban expressway—was selected as the study area (Figure 1A). The study area includes 7 administrative districts (including all of Dongcheng District and Xicheng District, as well as most of Chaoyang District, Haidian District, Fengtai District, and Shijingshan District and Daxing District), with a total area of approximately 667 km<sup>2</sup>.

## 2.2. Basic Data

The basic data used in the study included the road network dataset that was downloaded from the Open Street Map agency (OSM) [26], Baidu street view photos from the Baidu Map platform [27], satellite remote sensing imagery that was downloaded from European Space Agency (ESA), Beijing statistical yearbook data, and house price data that were obtained from a leading Chinese real estate agent. The details are as follows (Table 1).

Satellite imagery and the derived NDVI products (Figure 1C) were downloaded from the European Space Agency website [28]. The Sentinel imagery were obtained on June 14, 2017. The Sentinel-based NDVI dataset has a high spatial resolution (10 m) and is rapidly updated in time, making it ideal for urban study. Based on the application study provided by ESA in central Germany, the NDVI dataset has a high accuracy [31].

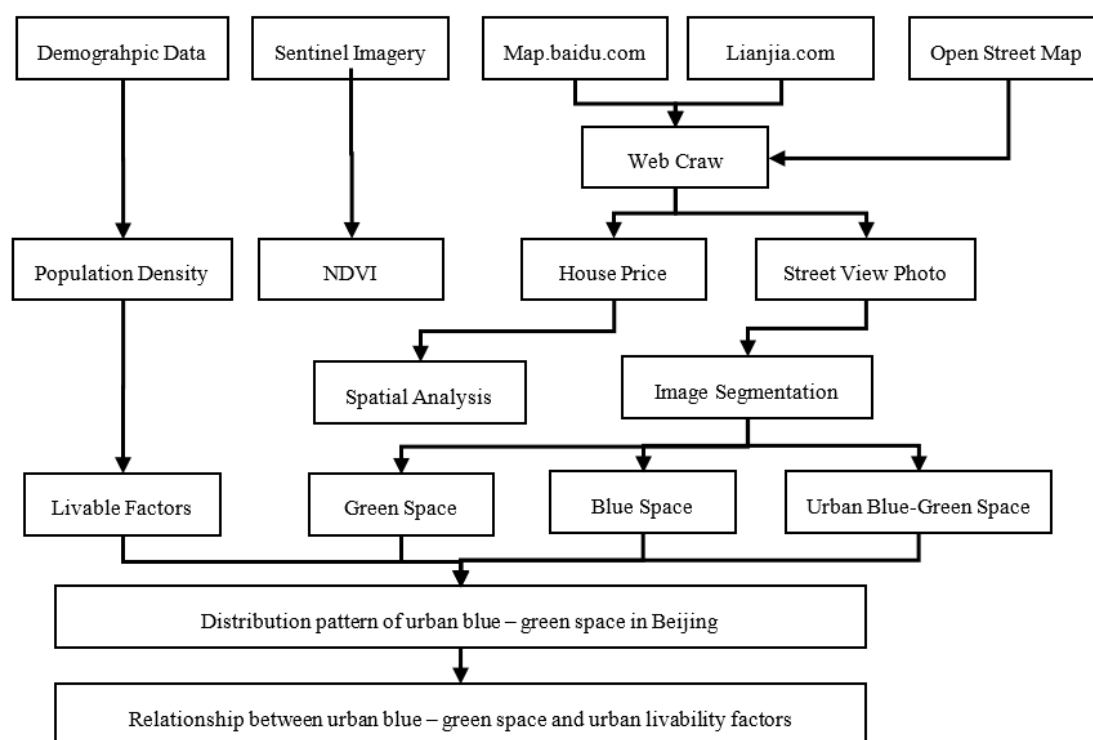
**Table 1.** Brief information about the datasets that were used in the study.

Data	Proportional Scale/Spatial Resolution	Year(s)	Data Sources
City Roads	—	Up to date	[26]
Street View Photos	300 dpi	Up to date	[27]
Satellite Imagery and NDVI	10 m	2017	[28]
Housing Transaction Data	—	2017	[29]
Statistical Data	—	2010	[30]

Housing price data were obtained from the website of Lianjia ([www.lianjia.com](http://www.lianjia.com), the largest real estate agent in China) [29]. By using the “Octopus” crawling system, the authors obtained information about 46,423 houses of Beijing in 2017, including the address and the price per unit area. Then, geocoding was applied to convert the address information into longitude and latitude information, and the above information was imported into ArcGIS to carry out spatial interpolation, forming a spatial map of housing prices in Beijing with a resolution of 200 m (Figure 1D).

### 2.3. Methods

The authors developed a program for capturing street view photos on the Baidu Map platform. The authors first designed a group of randomly distributed points in the study area and calculated the coordinates of all sample points. Based on coordinate information, 4 street view photos were obtained in each sample point from the Baidu Map platform by using a web crawler. Supported by the Image Cascade Network (ICNet) model and the Cityscapes scene dataset, the authors then carried content identification to obtain the blue sky and green vegetation objects. The authors counted the pixels of the blue and green objects and got the proportion values in each photo. Finally, the authors performed spatial interpolation in ArcGIS to obtain the spatial distribution map of the blue–green space area proportion index. The authors also performed a superposition analysis of the blue–green space area proportion index with social–economic factors, e.g., the NDVI, housing price, and population density. The technical flowchart is shown in Figure 2.

**Figure 2.** Technical flowchart of the study.

### 2.3.1. Obtain Street View Photos

In total, a set of 30,000 points was randomly selected in the study area, and the latitude and longitude coordinates of each point were extracted. Then, the street view photos were downloaded by using relevant Baidu street view map APIs (Application Programming Interface). The acquisition parameters of the street view photos are as follows: fovy (Field Of View Y-axis): 90; quality (picture quality): 95; heading (twist angle): initial value is 3.579°; add 90° each time; pitch (pitch angle): 0°; height: 512; and width: 1024. The authors downloaded a total of 97,451 street view photos. Typical street view photos are shown in Figure 3.

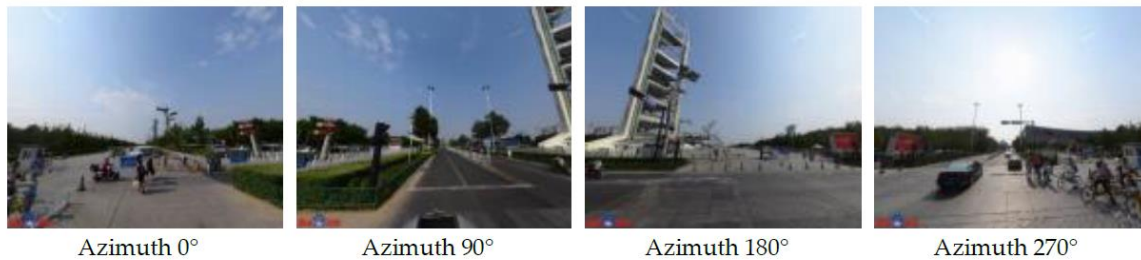


**Figure 3.** Typical street view photos. The scene location is 116.43° E, 39.92° N, near Linglong Tower, Olympic Park, Chaoyang District.

### 2.3.2. Identify Blue–Green Space

Based on the ICNet model and the Cityscapes scene dataset, the authors carried out image interpretation and recognition work supported by artificial intelligence. Cityscapes is a dataset of urban street view photos that are provided by the German Mercedes-Benz Auto Company, and the dataset can be downloaded from <https://www.cityscapes-dataset.com> [32]. Cityscapes contains street view photos in different scenes and seasons in 50 cities around the world, providing 5000 finely labeled images, 20,000 roughly labeled images, and 30 types of labeled objects. In this study, we divided the above scene dataset into 3 categories: a training sub-dataset, a validation sub-dataset, and a test sub-dataset, which contained 2975, 500, and 1525 photos, respectively.

Based on the classical PSPNet (Pyramid Scene Parsing Network) [33], the ICNet framework introduces the cascading feature fusion module to realize fast and high-quality image segmentation and semantic recognition. The model code can be downloaded from <https://github.com>. The basic process of image identification is as follows: Street view photos are first divided into three scale input models: low resolution, medium resolution, and high resolution. Low-resolution images were used for semantic extraction, and medium- and high-resolution images were used for the restoration and refinement of fuzzy boundaries. Considering both recognition accuracy and efficiency, ICNet has better segmentation accuracy and faster segmentation speed than the traditional PSPNet framework. Researchers have conducted comparisons on multiple datasets (Cityscapes, CamVid [34], COCO-stuff (Common Objects in Context [35]), and the results have shown that the ICNet model can identify the category elements well, and its segmentation accuracy (mIoU: Mean Intersection over Union) is about 69.5% [36].

After completing the training based on the Cityscapes dataset, the city street view photos of Beijing were inputted into the ICNet module with well-trained parameters to extract the blue sky and green vegetation objects, and then the pixel numbers of the two elements, the total pixel number of each photo, and the area proportion of the blue–green space were calculated. Finally, the blue–green space area proportions of the 4 pictures in each point were averaged to obtain the mean value. The specific formulas are as follows:

$$R_{BG} = \frac{N_b + N_g}{N} \times 100\% \quad (1)$$

$$R_B = \frac{N_b}{N} \times 100\% \quad (2)$$

$$R_G = \frac{N_g}{N} \times 100\% \quad (3)$$

where  $N_b$  is the number of pixels of the blue-sky object identified by the ICNet network,  $N_g$  is the number of pixels of the green vegetation object,  $N$  is the total number of pixels in each photo,  $R_B$  is the area proportion of blue space,  $R_G$  is the area proportion of green space, and  $R_{BG}$  is the area proportion of blue–green space.

### 2.3.3. Spatial Analysis in ArcGIS

In the study, the methods of kriging interpolation and geo-statistics analysis were also used supported by the ArcGIS platform. Kriging geospatial interpolation is an algorithm that considers the structural characteristics of the original values of the sample points and the variation function of the sample points in the region to make a linear optimal estimation of the values of the sample points [37]. In this study, the authors carried out kriging interpolation for the blue-sky space area proportion, green-vegetation space area proportion, blue–green space area proportion index, and housing price to get the planar map dataset from the point dataset.

The authors also applied the spatial analysis and geo-statistics analysis methods. Through these modules, on the one hand, the spatial distribution patterns of urban blue and green elements were demonstrated and analyzed via the visual approach. On the other hand, it was necessary to analyze the spatial correlation between urban blue–green space and the background social–economic and physical geographical factors. Geographically weighted regression (GWR) is a spatial extension of the ordinary linear regression model. In the GWR model, the regression coefficients of the explanatory variables are no longer constants but are rather functions of spatial position (called spatial weight functions). The GWR model can effectively capture spatial non-stationarity characteristics, and the NDVI, house price, and population density were selected as influencing factors in the GWR modeling process.

## 3. Results

### 3.1. The Spatial Distribution of Blue Space

The spatial distribution of the blue space area proportion index ( $R_B$ ) in Beijing and the statistics of different districts are shown in Figure 4.

The high-value areas of blue space were found to be mainly distributed in the western part of the city, with high topography and wide views, and the southern part of the city, with relatively backward urban development, fewer high-rise buildings, and lower floors (Figure 4a). For example, Summer Palace, Baoshan Village, Sijiqing Town, Fengtai Sports Center, Fengtai Science and Technology Park, Nanyuan Airport, and the areas along the urban expressway, viaducts, and golf clubs, are characterized with a high area proportion of blue space. In financial and business districts, science and technology parks, and areas within the Second Ring Road, such as Zhongguancun Science and Technology Park in Haidian District, Global Financial Center in Chaoyang District, Beijing 798 Art Park, and many historical protection areas within the Second Ring Road, the area proportion of blue space is significantly lower. These low-value areas usually have either large high-rise buildings or large low-rise buildings with narrow streets.

From the perspective of the administrative district dimension (Figure 4b), the average values of the blue space area proportion index, from highest to lowest, are as follows: Haidian District, Dongcheng District, Fengtai District, Xicheng District, Shijingshan District, Chaoyang District, and Daxing District. Located in the northwest of Beijing, Haidian District has the highest proportion index of blue space and exhibits the largest variation ( $0.062 \pm 0.035$ ). Daxing District, which is located in the southeast of Beijing, has the lowest proportion index and the lowest variability ( $0.038 \pm 0.016$ ). This result is related to the fact that Haidian District has many outdoor scenic spots, such as public parks and high-tech parks, while the section of Daxing District is characterized with high-density commercial buildings that were newly built in the 1990s. In the Beijing historical and cultural reserve zone (mainly within the

Second Ring Road of Beijing, including Dongcheng District and Xicheng District), the blue space area proportion index in Dongcheng District is significantly higher than that in Xicheng District. This result is closely related to the fact that most ministry-related buildings that were built in the 1950s are mainly located in Xicheng District.

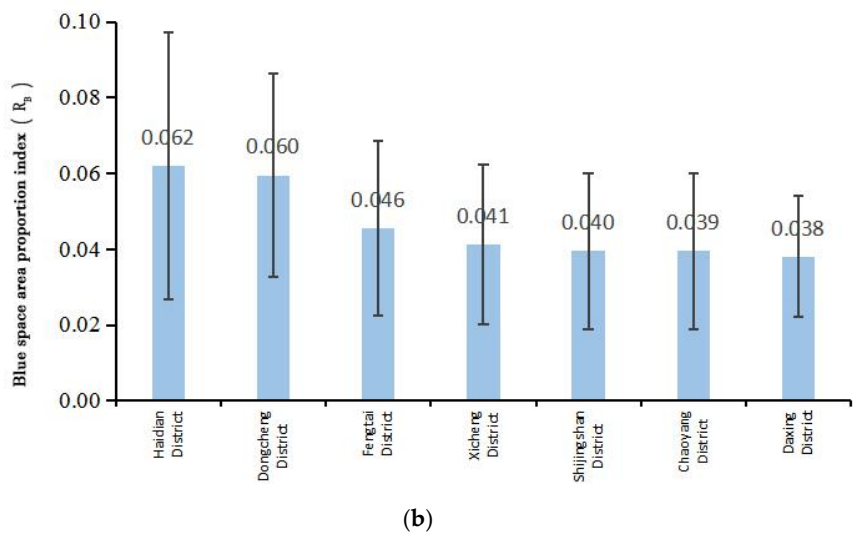
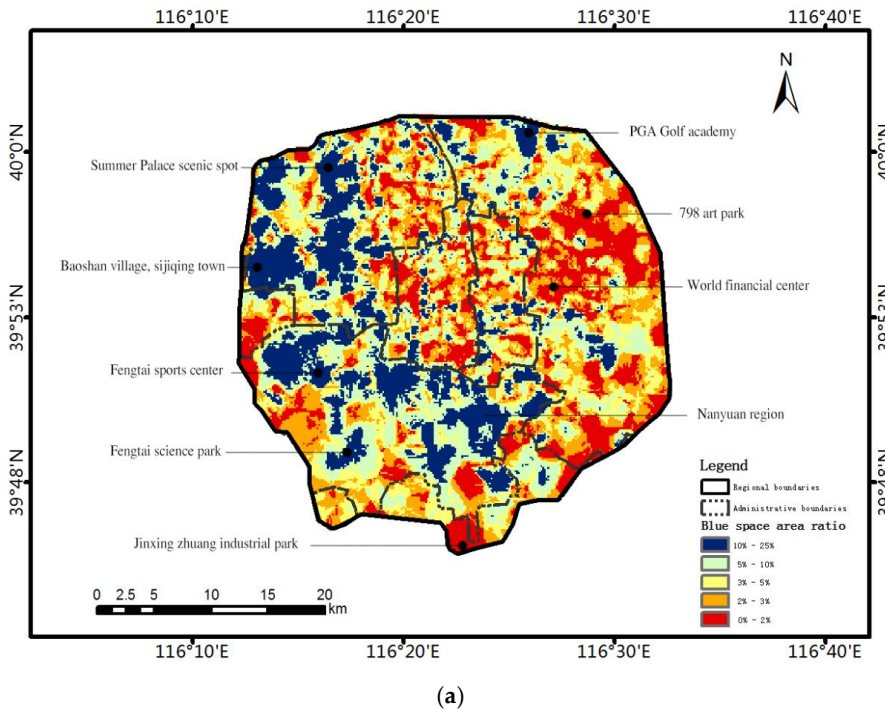


**Figure 4.** Spatial distribution of the blue space in Beijing. (a) Blue space area proportion index ( $R_B$ ) on a 200-m pixel; (b) statistics about blue space area proportion index ( $R_B$ ) in different districts.

### 3.2. The Spatial Distribution of Green Space

The spatial distribution of the green space area proportion index ( $R_G$ ) in Beijing and the statistics of different districts are shown in Figure 5.

The high-value areas of green space are mainly distributed in the west, north, and south of the city, but they are also in the southeast, northeast, and some core areas of the city; in contrast, the low-value areas of green space are mainly in the eastern and central regions of the city (Figure 5a). In places of

historic scene spots and country parks, such as the Summer Palace in Haidian District, the Olympic Park in Chaoyang District, the Forbidden City in the city center, the World Flower Garden in Fengtai District, and Wangxing Lake Country Park in Daxing District, the area proportion of urban green space is significantly higher. In financial business centers, highways, and transportation hubs, such as the Global Financial Center in Chaoyang District, the area of former Beijing Coking Plant, and Deshengmen area in Xicheng District, the area proportion of urban green space is significantly lower.

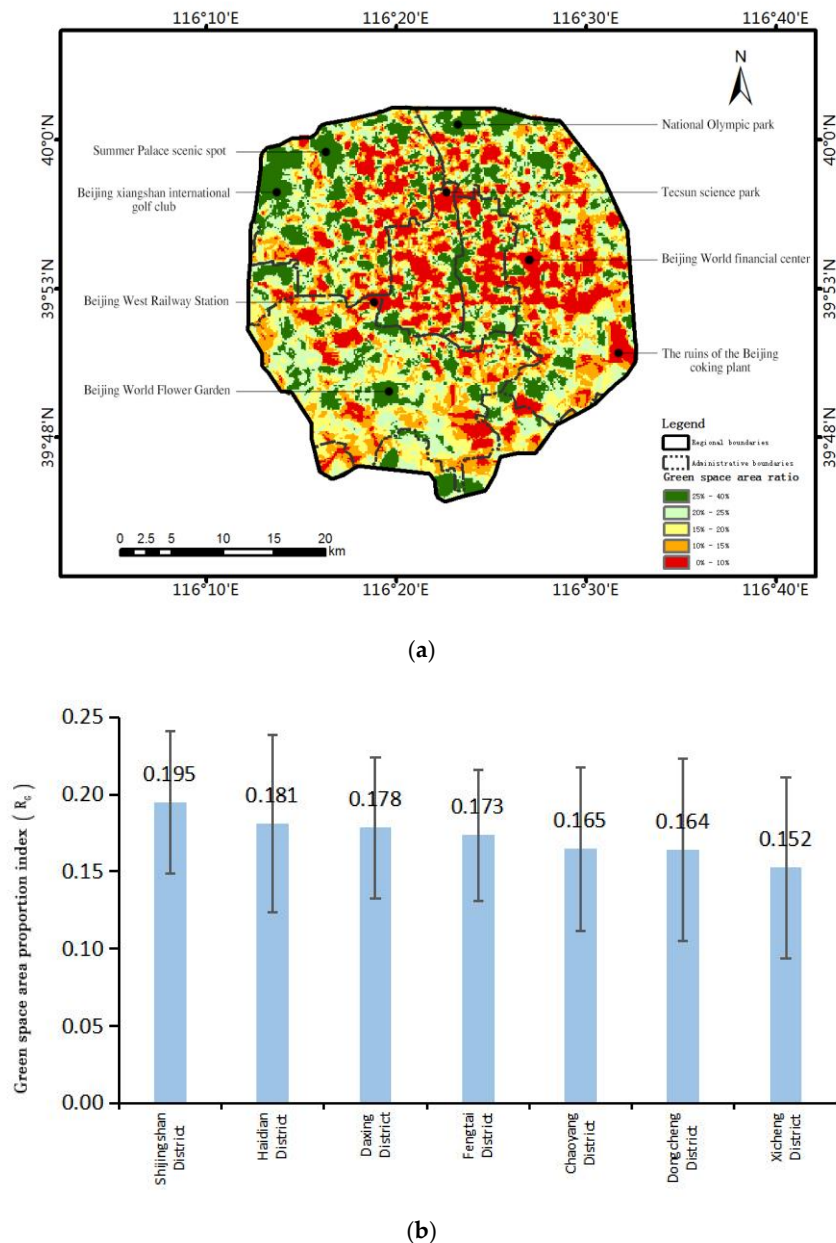


**Figure 5.** Spatial distribution of the green space in Beijing; (a) Green space area proportion index ( $R_G$ ) on a 200-m pixel scale; (b) statistics about green space area proportion index ( $R_G$ ) in different districts.

From the perspective of the administrative district dimension (Figure 5b), the average values of the green space area proportion index, from highest to lowest, are as follows: Shijingshan District, Haidian District, Daxing District, Fengtai District, Chaoyang District, Dongcheng District, and Xicheng District. The area of green space in Shijingshan District has the highest proportion index and the smallest variance ( $0.195 \pm 0.045$ ). Haidian District has a high proportion index ( $0.181 \pm 0.058$ ). Accordingly, in Dongcheng District and Xicheng District, which are the core areas of the city, the mean value of

street green space is small, and the variance is large (0.164 and 0.059 and 0.152 and 0.059, respectively). This result is related to the fact that Haidian District has many outdoor scene spots, parks, green spaces, colleges and universities, while many government affairs buildings and financial business buildings are distributed in Dongcheng District and Xicheng District.

### 3.3. The Spatial Distribution of Blue–Green Space

The spatial distribution of urban blue–green space area proportion index in Beijing ( $R_{BG}$ ) and spatial statistics based on city block scale are shown in Figure 6.

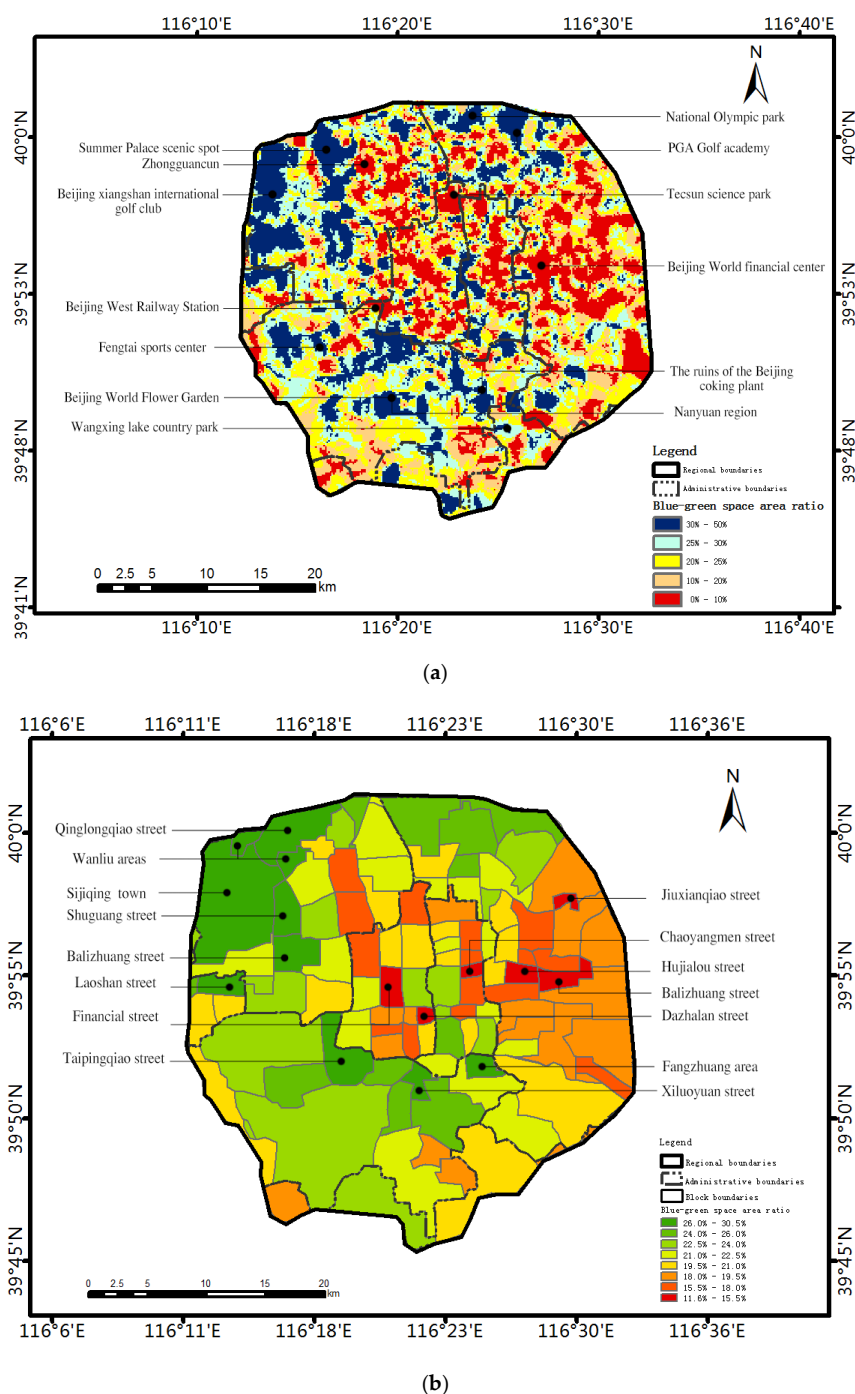


**Figure 6.** Spatial distribution of the blue–green space in Beijing. (a) blue–green space area proportion index ( $R_{BG}$ ) on a 200-m pixel scale; (b) blue–green space area proportion index ( $R_{BG}$ ) on a city block scale.

The spatial distribution pattern of blue–green space area proportion index in Beijing shows an increasing trend from east to west; the spatial distribution of blue–green space has a close spatial relationship with the natural environment and regional social–economic development. The distribution of the blue–green space area proportion index is basically the same as that of the green space area proportion index.

On the city block scale, the urban blue–green space area accounts for a high proportion of areas in Haidian District (Wanliu Block, Qinglongqiao Block, Shuguang Block, Balizhuang Block, Sijiqing Town), Fengtai District (Fangzhuang Block, Taipingqiao Block, West Luoyuan Block), and Shijingshan District (Laoshan Block). Low-value locations are in Chaoyang District (Jiuxianqiao Block, Hujialou Block, Balizhuang Block), Xicheng District (Dashilan Block, Finance Street Block), and Dongcheng District (Chaoyangmen Block). Among them, the highest region is Shuguang Block, which is located in the hinterland of Haidian District, with a blue–green space area proportion of 30.1%. The lowest region is Hujialou Block, which is located in the prosperous Central Business District of Chaoyang District, Beijing, with a blue–green space area proportion of 11.6%.

### 3.4. The Relationship Between Green Space and the NDVI

At different spatial scales (500 m, 1000 m, and street scales), GWR analysis was performed for the vegetation index (NDVI) based on satellite remote sensing images and the green space area proportion index ( $R_G$ ) based on streetscape photos (Figure 7).

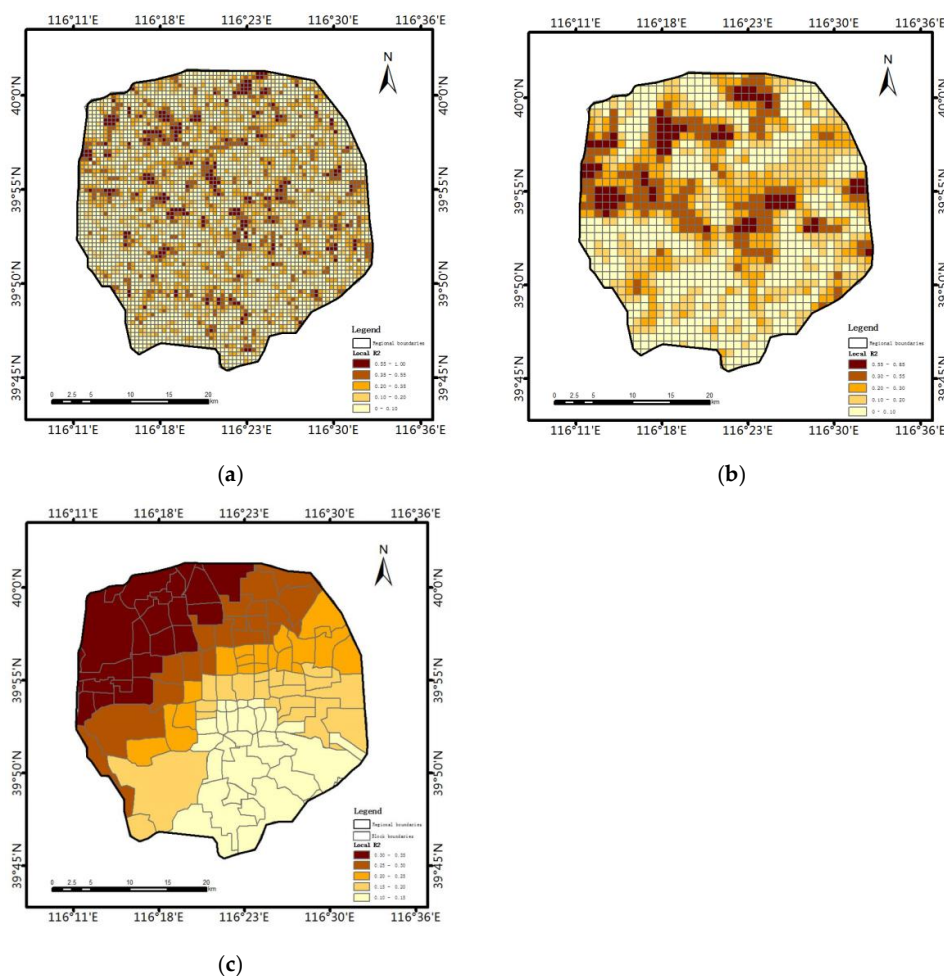


**Figure 7.** Spatial distribution of fitting degrees between the NDVI and green space area proportion index ( $R_G$ ); The pixel scale is 500 m (a), 1000 m (b), and city block (approximately 2000–20,000 m) (c) respectively.

The results showed that there was a positive correlation between the satellite remote sensing NDVI and green space area proportion index ( $R_G$ ), but the fitting degree of GWR decreased as the analysis scale increased. At the 500 m pixel scale, the adjusted fitting degree ( $R^2 = 0.73$ ) was the largest. At the 1000 m pixel scale, the adjusted fitting degree ( $R^2 = 0.50$ ) decreased. At the city block scale (approximately 2000–20,000 m), the adjusted fitting degree ( $R^2 = 0.30$ ) was the smallest. In general (Figure 7c), the regression effects of the satellite remote sensing NDVI and green space area proportion index ( $R_G$ ) in the northwestern part of the city were the best. The southern part of the city had the worst regression effect. However, at finer scales, such as the 500 m scale shown in Figure 7a and the 1000 m scale shown in Figure 7b, the areas with better spatial fitting degree were distributed loosely in most regions.

### 3.5. The Relationship Between Blue–Green Space and Housing Price

The authors analyzed the correlation between the area proportion index of blue–green space and urban housing price. The results showed that within the Third Ring Road in Beijing, the two were negatively correlated ( $r = -0.293$ ,  $p = 0.01$ ); however, outside of the Third Ring Road, they were positively correlated ( $r = 0.119$ ,  $p = 0.01$ ).

The reason for this difference may be that most of the areas within the Third Ring Road belong to historical and cultural protection zones, areas that are related to government affairs or high-level commerce affairs. The price of residential housing is mainly affected by the functions of the block (e.g., business districts, government districts, and ordinary residential areas) or the scarcity of specific resources (e.g., school district housing), but it has little to do with the ecological environment. The areas between the Third Ring Road and the Fifth Ring Road do not have strong urban functional attributes, and the land resources that are available for future development are relatively abundant with fewer constraints. Therefore, the house price has a significant synchronization effects with ecological quality (i.e., the area proportion index of blue–green space).

Similarly, on different spatial scales (500 m, 1000 m, and block scales), the authors performed GWR analysis on the ratio of house prices to the blue–green space area proportion index (Figure 8). The results showed that although there were different relationships (positive or negative correlation) between housing prices and blue–green space in different regions, the fitting degree of the two increased with the increase of analysis scale. At the 500 m pixel scale, the adjusted fitting degree ( $R^2 = 0.28$ ) was the smallest. At the 1000 m pixel scale, the adjusted fitting degree ( $R^2 = 0.33$ ) increased. At the city block scale (approximately 2000–20,000 m), the adjusted fitting degree ( $R^2 = 0.41$ ) was the largest. In terms of spatial perspective (Figure 8c), among the areas within the Third Ring Road, the best fitting degrees were obtained from Yangfangdian Block in Haidian District, Taipingqiao Block in Fengtai District, You'anmen Block, and Guang'anmenwai Block in Xicheng District. In the areas outside the Third Ring Road, the spatial fits of Yayuncun Block, Xiaoguan Block, and Datun Block in Chaoyang District were the highest.

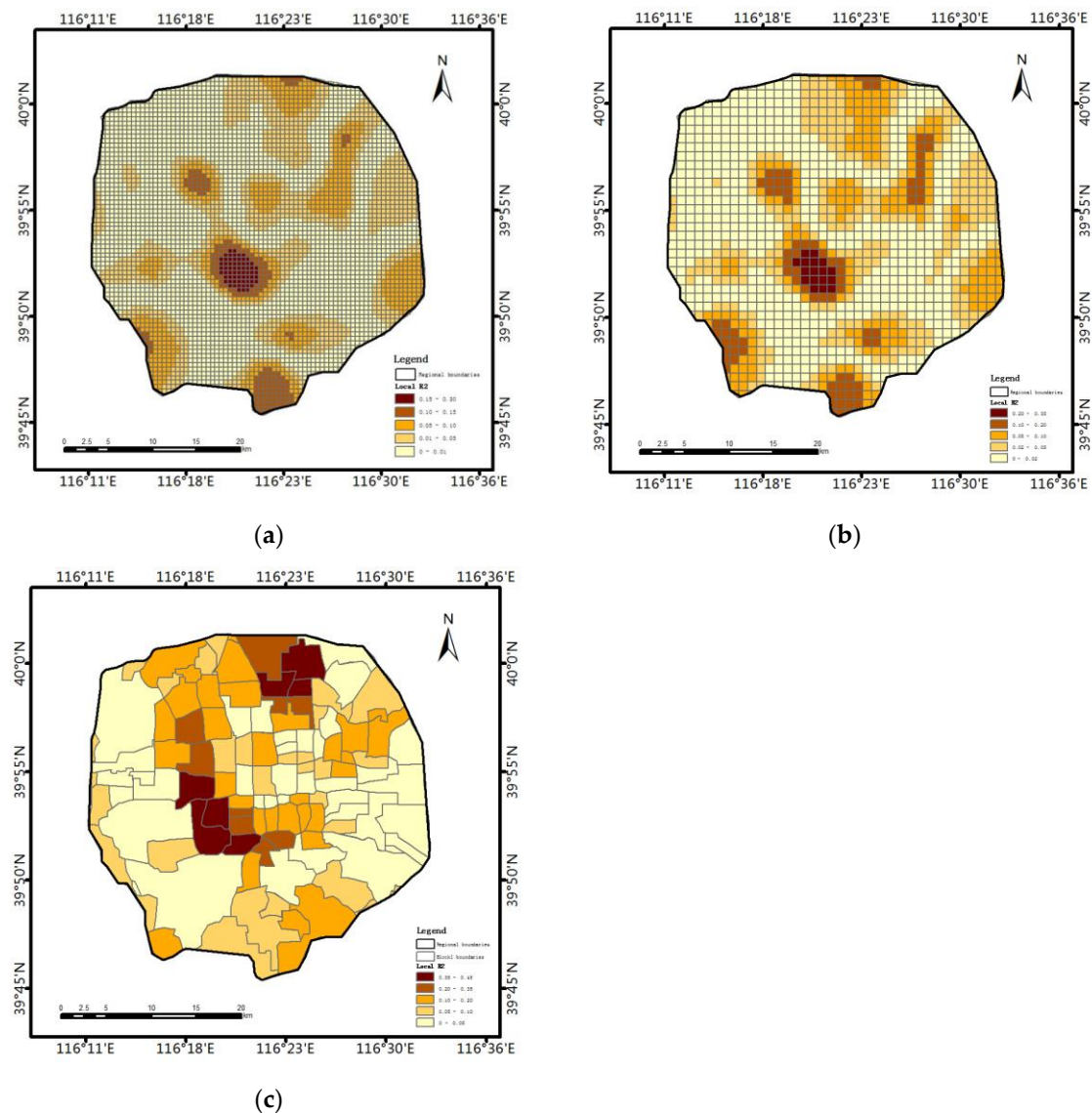
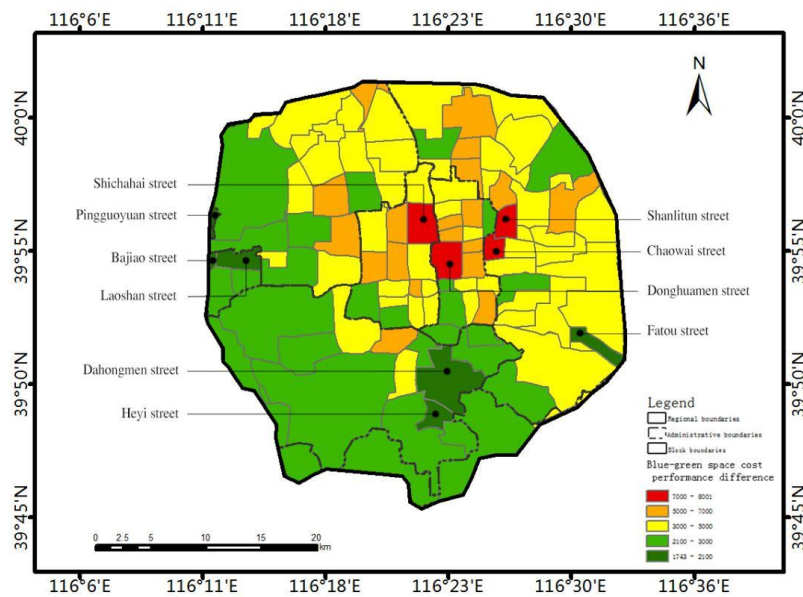
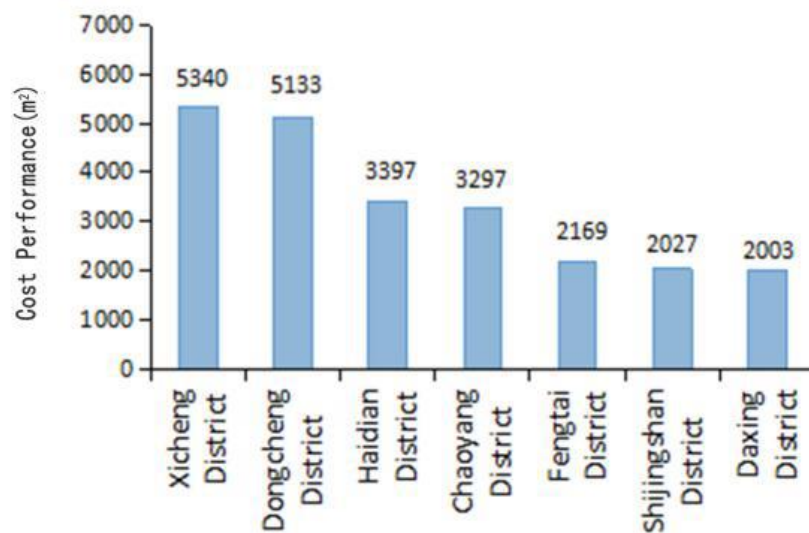


**Figure 8.** Spatial distribution of fitting degrees of urban housing price and blue-green space area proportion index; The pixel scale is 500 m (a), 1000 m (b), and city block (approximately 2000–20,000 m) (c), respectively.

On the block scale, the ratio of house prices to the area proportion index of blue-green space was calculated, and the results (Figure 9a) showed that the blue-green space in the western and southern parts of the city, such as Pingguoyuan Block, Laoshan Block, Bajiao Block, Heyi Block, Dahongmen Block, and Fatou Block, has the highest cost-effectiveness. However, the blue-green space in the northern and eastern regions was found to be in the middle in terms of cost performance. The blue-green space in the core areas of the city, such as Shichahai Block, Donghuamen Block, Chaowai Block, and Sanlitun Block, was found to have the lowest cost performance. From the perspective of the administrative district (Figure 9b), the housing prices corresponding to the area proportion index of the blue-green space were found as follows: Xicheng District, Dongcheng District, Haidian District, Chaoyang District, Fengtai District, Shijingshan District, and Daxing District.



(a)



(b)

**Figure 9.** Cost performance of blue–green space. (a) The housing price corresponding to the ratio of unit blue–green space area based on block statistics (housing unit price/ratio of blue–green space area); (b) the housing price corresponding to the percentage of blue–green space per unit based on administrative statistics.

### 3.6. The Relationship Between Blue–Green Space and Population Density

Because population data were not rasterized on pixel level, the analysis of the relationship between blue–green space area proportion index and population density was performed on the block scale. The analysis showed that on the city block scale, the urban blue–green space area proportion index and population density showed a negative correlation ( $r = -0.259$ ,  $p = 0.01$ ). The fitting degree of spatial regression reached 0.44 (Figure 10). This result indicates that the larger the population per unit area is, the lower the area proportion index of blue–green space is. The reason for this relationship is that larger block populations need more residential, commercial, and transportation facilities, and housing construction will be more concentrated because space that can be provided for ecological construction will be limited.

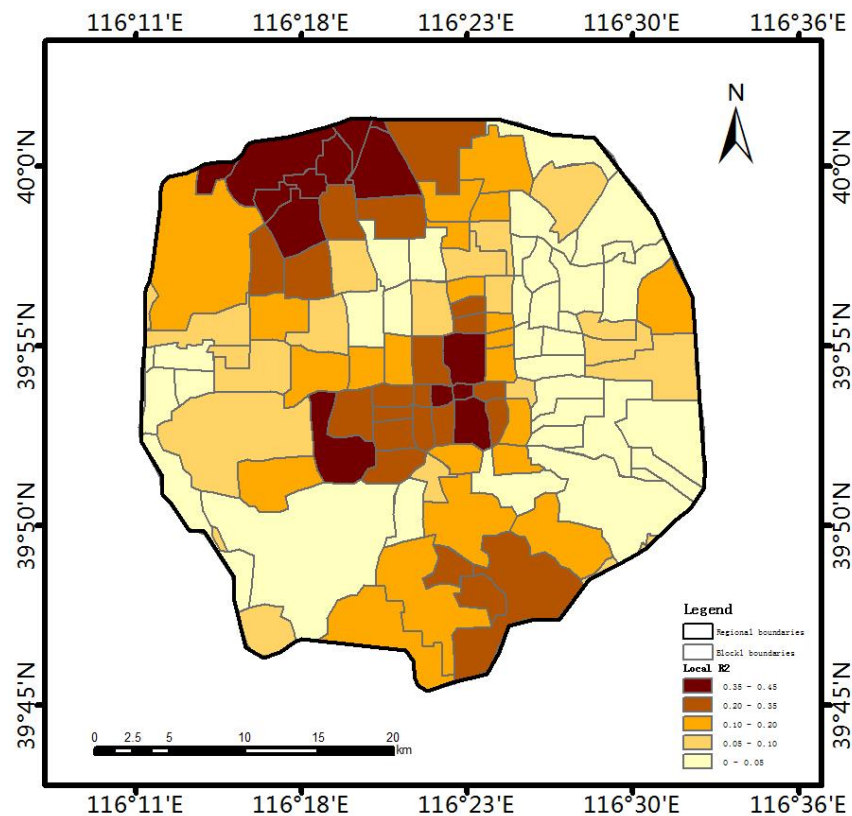
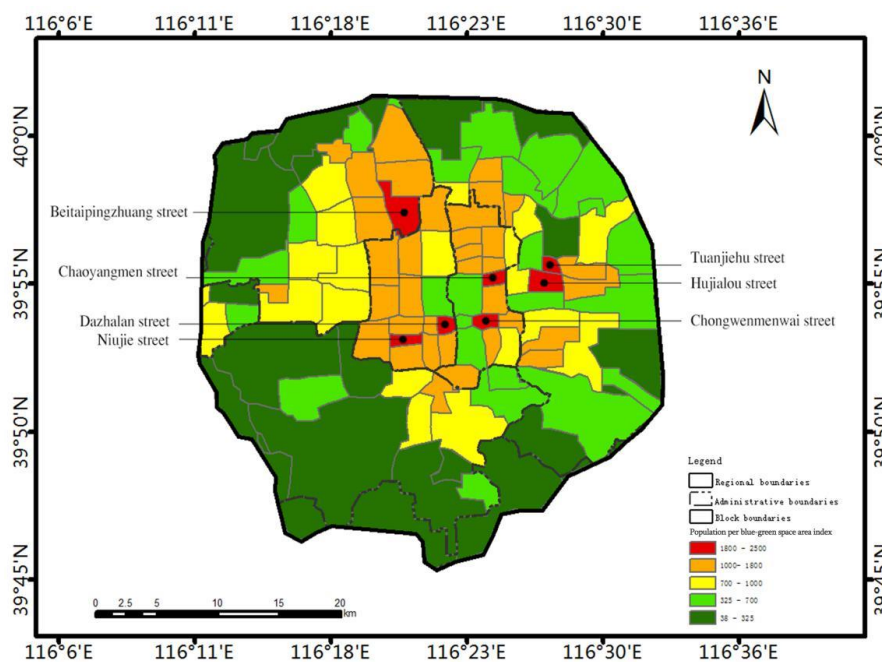
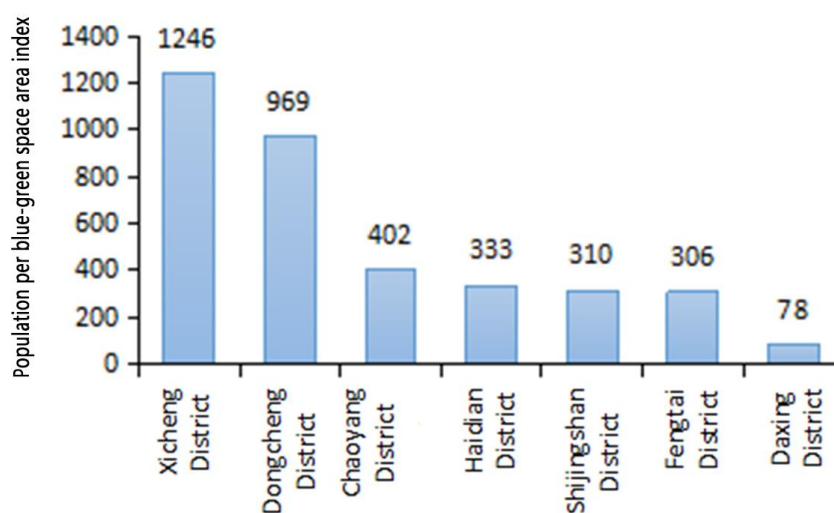


Figure 10. Spatial fitting degree between urban population density and blue–green space.

The authors calculated the ratio of the population to the area proportion index of blue–green space on the block scale. The results (Figure 11) showed that the low-population per blue–green space is mainly distributed in the southern part of the city and the fringe areas outside the Third Ring Road, e.g., Pingguoyuan Block, Guang’anmenwai Block, Niujie Block, Chaoyangmen Block, Chongwenmenwai Block, Hujialou Block, Beitaipingzhuang Block, and Tuanjiehu Block. The high-population density per blue–green space includes Beitaipingzhuang Block, Niujie Block, Dashilan Block, Chongwenmenwai Block, Chaoyangmen Block, Tuanjiehu Block, and Hujialou Block. From the perspective of the administrative area, the ratio of the population density to the blue–green space area index, from high to low, is Xicheng District, Dongcheng District, Chaoyang District, Haidian District, Shijingshan District, Fengtai District, and Daxing District.



(a)



(b)

**Figure 11.** Spatial distribution of population density per blue–green space area proportion index. (a) Spatial distribution in different city block; (b) Statistics in different districts.

## 4. Discussion

### 4.1. Significances

The traditional “top–down” satellite monitoring study has the advantages of being fast and objective observation methods. However, it also has the disadvantage of having less connection with residents’ intuitive visual perceptions. This study based on street view photos hopes to describe and reconstruct the living environment from the perspective of ordinary residents. Street view photos were used to directly extract key environmental information to describe and simulate urban environmental conditions. The research results can be used to guide the environmental planning and construction work. For policy makers and planners in the construction of new urban areas or the reconstruction of

old urban areas, in order to enhance the vitality and sustainability of the city, more attention should be paid to the design and construction of blue–green spaces to improve the well-being of residents.

Our study shows that on different scales, there is a difference in the correlation between the area proportion index of green space and the NDVI value. There is a weak correlation on the pixel scale, which is consistent with many other studies [38,39]. However, the fitting degree of geospatial weighted regression decreases at increasing scales, which represents significant progress compared with previous studies. Our study found that the high-value area of Beijing’s blue–green space has a good spatial correspondence with the city’s places of interest, public parks, and newly constructed buildings (especially after the 2000s). However, the low-value area of blue–green space has a good spatial correspondence with the historical and cultural buildings that are located in the core of the city and the construction areas mainly built in the last century (especially before 1970s). This reflects the relationship between blue–green space, urban land functions, and urban development.

#### 4.2. Uncertainties

First, to reduce the distortion of the street view photos, the authors set the vertical and horizontal widths in each picture to a 90° viewing angle. However, there are differences between the above settings and the actual viewing angles of human beings (the upper and lower widths are approximately 130°, and the left and right widths are approximately 156°) [40]. Since human eyes have a larger and wider angle of view, the area of blue space that is obtained by the retina of the human eye accounts for a larger proportion than the results obtained in this paper.

Second, the photo views are different for the street drivers and the side walkers. In order to reduce the impacts that were induced by this minor difference, this article first used street view photos in four directions to calculate the blue–green space area proportion index. At the same time, the authors would like to emphasize that this study did not particularly care about the absolute value of urban blue–green space area proportion, and we were more concerned about the spatial distribution rules and their formation mechanism. Therefore, considering the above two factors, even when the shooting location was not a sidewalk, the technical route that was constructed in this article was still robust, and the relevant conclusions are valid and scientific.

Thirdly, street view photos may vary greatly on different seasons or dates. For a megalopolis such as Beijing, street view photos might be taken in different years, different seasons, different and weather conditions, all of which will affect photo quality. In particular, the different seasons lead to large differences in the extraction and calculation of green space, and atmospheric pollution conditions will affect the extraction and calculation of blue space. Overall, street view photos in winter reduce green space and slightly increase blue space. During cloudy days or days with severe air pollution events, the extraction process of green space and blue space is dramatically reduced.

In addition, the ICNet artificial neural network and Cityscapes scene dataset were used in this article. The above mature neural network model and scene dataset have been applied in many studies, and previous studies have proven that the ICNet model can well-identify the different elements in street view photos, and its segmentation accuracy (mIoU) reaches 69.5% [28]. There is no doubt that the recognition accuracy of ICNet model and the labelling accuracy of Cityscapes dataset affected the accuracy of this paper. All these elements need to be further improved in future study.

## 5. Conclusions

In this study, by using web crawler and geographic spatial analysis technology, the ICNet model and Cityscapes dataset were applied to carry out blue–green space identification and geo-statistical analysis in Beijing. The authors constructed a set of technical frameworks, summarized the distribution pattern of blue–green space, and analyzed the relationships between the blue–green space information and many environmental factors.

The study showed that the spatial distribution of the area proportion index of blue–green space in Beijing was higher in the west and lower in the middle and east. The high-value area of the blue and

green space area proportion index had spatial correspondence with scenic spots and historical sites, parks and green spaces, and buildings that were constructed in different ages. At the pixel scale, the correlation between blue–green space and the NDVI was weak, but at the city block scale, the correlation between the two was good. The area proportion index of blue–green space was also closely related to housing prices and population density.

This study provided new ideas for the monitoring and evaluation of urban ecosystems. At present, the extraction and analysis frame still has some problems, e.g., obtaining the time stamp of street view photos, modeling the same perspective observation range as human beings, and improving the detection accuracy of blue–green space. In the future, in-depth and more accurate analysis should be carried out to address the above problems.

**Author Contributions:** Y.H. designed and supervised the study. H.W. and L.T. performed the experiments, Y.H., H.W., L.T. and Q.Z. preliminarily analyzed the results. All authors drafted and revised the paper. All authors have read and agreed to the published version of the manuscript.

**Funding:** Strategic Priority Research Program of Chinese Academy of Sciences, Grant Numbers: XDA23100200, XDA20010202, XDA19040301; National Key Research and Development Plan Program in China, Grant Numbers: 2016YFB0501502, 2016YFC0503701.

**Conflicts of Interest:** The authors declare no conflicts of interest.

## References

- Leggett, J.A.; Carter, N.T. Rio+20: The United Nations Conference on Sustainable Development. June 2012. Available online: <https://digital.library.unt.edu/ark:/67531/metadc93939> (accessed on 1 September 2019).
- Wu, D.; Wang, Y.; Fan, C.; Xia, B. Thermal environment effects and interactions of reservoirs and forests as urban blue-green infrastructures. *Ecol. Indic.* **2018**, *91*, 657–663. [[CrossRef](#)]
- Ahmed, S.; Meenar, M.; Alam, A. Designing a Blue-Green Infrastructure (BGI) Network: Toward Water-Sensitive Urban Growth Planning in Dhaka, Bangladesh. *Land* **2019**, *8*, 138. [[CrossRef](#)]
- Zhou, Y.; Shi, T.; Hu, Y.; Gao, C.; Liu, M.; Fu, S.; Wang, S. Urban green space planning based on computational fluid dynamics model and landscape ecology principle: A case study of Liaoyang City, Northeast China. *Chin. Geogr. Sci.* **2011**, *21*, 465–475. [[CrossRef](#)]
- Sander, H.A.; Zhao, C. Urban green and blue: Who values what and where? *Land Use Policy* **2015**, *42*, 194–209. [[CrossRef](#)]
- Vaeztavakoli, A.; Lak, A.; Yigitcanlar, T. Blue and Green Spaces as Therapeutic Landscapes: Health Effects of Urban Water Canal Areas of Isfahan. *Sustainability* **2018**, *10*, 4010. [[CrossRef](#)]
- Liu, Y.; Wang, R.; Grekousis, G.; Liu, Y.; Yuan, Y.; Li, Z. Neighbourhood greenness and mental wellbeing in Guangzhou, China: What are the pathways? *Landsc. Urban Plan.* **2019**, *190*, 103602. [[CrossRef](#)]
- Vich, G.; Marquet, O.; Miralles-Guasch, C. Green streetscape and walking: Exploring active mobility patterns in dense and compact cities. *J. Transp. Heal.* **2019**, *12*, 50–59. [[CrossRef](#)]
- Hu, Y.; Zhao, G.; Zhang, Y. Analysis of spatial and temporal dynamics of green coverage and vegetation greenness in Beijing. *J. Geo-Inf. Sci.* **2018**, *20*, 332–339.
- Puissant, A.; Rougier, S.; Stumpf, A. Object-oriented mapping of urban trees using Random Forest classifiers. *Int. J. Appl. Earth Obs. Geoinf.* **2014**, *26*, 235–245. [[CrossRef](#)]
- Schreyer, J.; Lakes, T. Tandem-x & uav data for modeling 3d vegetation information in urban areas. In Proceedings of the 2015 Joint Urban Remote Sensing Event (JURSE), Lausanne, Switzerland, 30 March–1 April 2015; pp. 1–4.
- Liu, Y.; Chen, Y.; Yue, D.; Feng, Z. Information extraction of urban green space based on uav remote sensing image. *Sci. Surv. Mapp.* **2017**, *42*, 59–64.
- Zhang, H.; Zhu, S.; Wang, M.; Zhang, Z.; Zhang, G. Sky view factor estimation based on 3d urban building data and its application in urban heat island—Illustrated by the case of Adelaide. *Remote Sens. Technol. Appl.* **2015**, *30*.
- Manandhar, D.; Shibasaki, R. Vehicle-borne laser mapping system (VLMS) for 3-D GIS. In Proceedings of the IEEE 2001 International Geoscience and Remote Sensing Symposium (Cat. No.01CH37217), Scanning the Present and Resolving the Future, Sydney, NSW, Australia, 9–13 July 2001; Volume 5, pp. 2073–2075.

15. Hao, X.; Long, Y. Street greenery: A new indicator for evaluating walkability. *Shanghai Urban Plan. Rev.* **2017**, *1*, 32–36.
16. Zhao, Q.; Tang, H.; Wei, D.; Wanhui, Q. Spatial visibility of green areas of urban greenway using the green appearance percentage. *J. Zhejiang A F Univ.* **2016**, *33*, 288–294.
17. Jiang, B.; Deal, B.; Pan, H.; Larsen, L.; Hsieh, C.-H.; Chang, C.-Y.; Sullivan, W.C. Remotely-sensed imagery vs. eye-level photography: Evaluating associations among measurements of tree cover density. *Landsc. Urban Plan.* **2017**, *157*, 270–281. [[CrossRef](#)]
18. Yang, J.; Zhao, L.; McBride, J.; Gong, P. Can you see green? Assessing the visibility of urban forests in cities. *Landsc. Urban Plan.* **2009**, *91*, 97–104. [[CrossRef](#)]
19. Zhang, L.; Pei, T.; Chen, Y.; Song, C.; Liu, X. A review of urban environmental assessment based on street view images. *J. Geo-Inf. Sci.* **2019**, *21*, 46–58.
20. Hu, Y.; Zhang, Q.; Zhang, Y.; Yan, H. A Deep Convolution Neural Network Method for Land Cover Mapping: A Case Study of Qinhuangdao, China. *Remote Sens.* **2018**, *10*, 2053. [[CrossRef](#)]
21. Chen, S.; Wang, H. SAR target recognition based on deep learning. In Proceedings of the 2014 International Conference on Data Science and Advanced Analytics (DSAA), Shanghai, China, 30 October–1 November 2014; pp. 541–547.
22. Navickas, L.; Olszewska, A.; Mantadelis, T. Class: Contemplative landscape automated scoring system. In Proceedings of the 2016 24th Mediterranean Conference on Control and Automation (MED), Athens, Greece, 21–24 June 2016; pp. 1180–1185.
23. Wang, R.; Lu, Y.; Zhang, J.; Liu, P.; Yao, Y.; Liu, Y. The relationship between visual enclosure for neighbourhood street walkability and elders' mental health in China: Using street view images. *J. Transp. Health* **2019**, *13*, 90–102. [[CrossRef](#)]
24. GaWC. The World according to GAWC 2018. Available online: <https://www.lboro.ac.uk/gawc/world2018t.html> (accessed on 1 September 2019).
25. China Statistical Yearbook 2018. Available online: <http://www.stats.gov.cn/tjsj/ndsj/2018/indexeh.htm> (accessed on 1 September 2019).
26. Open Street Map. Available online: <https://www.openstreetmap.org/> (accessed on 1 September 2019).
27. Baidu Map Platform. Available online: <https://map.baidu.com/> (accessed on 1 September 2019).
28. European Space Agency. Available online: <https://earth.esa.int/web/sentinel/user-guides/sentinel-2-msi/product-types/level-1c/> (accessed on 1 September 2019).
29. Homepage of Lianjia Company. Available online: <https://bj.lianjia.com/> (accessed on 1 September 2019).
30. Yearbook of China. Available online: <http://www.yearbookchina.com/> (accessed on 1 September 2019).
31. Lange, M.; DeChant, B.; Rebmann, C.; Vohland, M.; Cuntz, M.; Doktor, D. Validating MODIS and Sentinel-2 NDVI Products at a Temperate Deciduous Forest Site Using Two Independent Ground-Based Sensors. *Sensors* **2017**, *17*, 1855. [[CrossRef](#)]
32. Cordts, M.; Omran, M.; Ramos, S.; Rehfeld, T.; Enzweiler, M.; Benenson, R.; Franke, U.; Roth, S.; Schiele, B. The Cityscapes Dataset for Semantic Urban Scene Understanding. In Proceedings of the 2016 IEEE Conference on Computer Vision and Pattern Recognition (CVPR), Las Vegas, NV, USA, 27–30 June 2016; pp. 3213–3223.
33. Zhao, H.; Shi, J.; Qi, X.; Wang, X.; Jia, J. Pyramid scene parsing network. In Proceedings of the 2017 IEEE Conference on Computer Vision and Pattern Recognition (CVPR), Honolulu, HI, USA, 21–26 July 2017; pp. 6230–6239.
34. Brostow, G.J.; Fauqueur, J.; Cipolla, R. Semantic object classes in video: A high-definition ground truth database. *Pattern Recognit. Lett.* **2009**, *30*, 88–97. [[CrossRef](#)]
35. Caesar, H.; Uijlings, J.; Ferrari, V. COCO-Stuff: Thing and Stuff Classes in Context. In Proceedings of the 2018 IEEE/CVF Conference on Computer Vision and Pattern Recognition, Salt Lake City, UT, USA, 18–23 June 2018; pp. 1209–1218.
36. Zhao, H.; Qi, X.; Shen, X.; Shi, J.; Jia, J. ICNet for Real-Time Semantic Segmentation on High-Resolution Images. *arXiv* **2017**, arXiv:1704.08545.
37. Marinoni, O. Improving geological models using a combined ordinary–indicator kriging approach. *Eng. Geol.* **2003**, *69*, 37–45. [[CrossRef](#)]
38. Ye, Y.; Zhang, L.; Yan, W.; Zeng, W. Measuring street greening quality from humanistic perspective: A large-scale analysis based on Baidu street view images and machine learning algorithms. *Landsc. Archit.* **2018**, *25*, 24–29.

39. Helbich, M.; Yao, Y.; Liu, Y.; Zhang, J.; Liu, P.; Wang, R. Using deep learning to examine street view green and blue spaces and their associations with geriatric depression in Beijing, China. *Environ. Int.* **2019**, *126*, 107–117. [[CrossRef](#)]
40. Cheng, L.; Chu, S.; Zong, W.; Li, S.; Wu, J.; Li, M. Use of Tencent Street View Imagery for Visual Perception of Streets. *ISPRS Int. J. Geo-Inf.* **2017**, *6*, 265. [[CrossRef](#)]



© 2020 by the authors. Licensee MDPI, Basel, Switzerland. This article is an open access article distributed under the terms and conditions of the Creative Commons Attribution (CC BY) license (<http://creativecommons.org/licenses/by/4.0/>).